https://doi.org/10.5194/essd-2024-503
Preprint. Discussion started: 25 November 2024
© Author(s) 2024. CC BY 4.0 License.

Open Access Earth System Science Data Discussions

Global spatially-distributed sectoral GDP map for disaster risk analysis

Takeshi Shoji[1,2], Dai Yamazaki[1,2], Yuki Kita[2,3], Megumi Watanabe[2,4]

[1]Graduate School of Engineering, The University of Tokyo, Tokyo, 113-8656, Japan
[2]Institute of Industrial Science, The University of Tokyo, Tokyo, 153-8505, Japan
[3]Gaia Vision Inc., Tokyo, Japan
[4]LERMA, Observatoire de Paris, Paris, 75014, France

Correspondence to: Takeshi Shoji (tshoji@rainbow.iis.u-tokyo.ac.jp)

Abstract. Global risk assessments of economic losses by natural disasters while considering various land uses is essential. However, sector-specific, high-resolution pixel-level economic data are not yet available globally to assess exposure to local disasters such as floods. In this study, we employed new land-use data to construct global, spatially distributed map of sector-specific gross domestic product (GDP). We developed three global GDP maps in 2010, 2015, and 2020 for service, industry, and agriculture sector, with 30 arcsec resolution. Firstly, we found that the spatial relationship between the distribution of industrial GDP and urban areas, where the service GDP is highly concentrated, varies across countries. For example, in the United States, industrial GDP is widely dispersed regardless of urban areas, whereas in India, industrial GDP is concentrated in proximity to urban areas. Secondly, we evaluated the GDP map by subnational regional statistics of Thailand, where validation data are accessible. Traditional GDP maps relying solely on population distribution exhibited 63.0% relative error of the sectoral GDP in each subnational region to regional statistical data, which the new sector-specific GDP map reduced to 26.2%. Subsequently, we assessed the map in conjunction with sector-level business interruption (BI) losses resulting from river flooding. Our estimation of sector-level losses revealed that the sectoral ratio to the total loss varied significantly depending on the spatial distribution of flood hazards. The estimated total loss became closer to the reported value when the new GDP map was used, while sectoral ratios of losses still had some differences from the reported ratios suggesting the need for further improving the procedures of loss-estimation models. These global sectoral GDP maps (SectGDP30) are available at https://doi.org/10.5281/zenodo.13991673 (Shoji et al., 2024).

1 Introduction

In recent years, as natural disasters have become more frequent and found throughout the world (IPCC, 2012), global spatial data including land use and socioeconomic information have become essential for estimating the extent of disaster damage and losses. With the increasing frequency and impact of localized natural disasters such as floods, high-resolution data

https://doi.org/10.5194/essd-2024-503
Preprint. Discussion started: 25 November 2024
© Author(s) 2024. CC BY 4.0 License.

capturing the spatial distribution of socioeconomic factors are essential. However, socioeconomic data published by international organizations such as the World Bank are often available only at the national or large municipal level. At the research level, economic data at the municipal level have been studied (Wenz et al., 2023); however, obtaining grid-level data at a resolution of several kilometers has been still challenging.

For example, as for the impact-assessment of flood disasters, researchers have undertaken a series of studies by spatially calculating the amount of asset quantity and production activity overlapped with inundated areas, leveraging global maps. Achieving this necessitates the downscaling of national-level data of economic activity, mainly gross domestic product (GDP), to finer subnational or grid-based levels. This type of product by downscaling GDP is called a "spatially distributed GDP map". This downscaling practice typically relies on gridded population data (Tanoue et al., 2021; Willner et al., 2018). Alternatively, it has involved the assembly and interpolation of available subnational statistics (Duan et al., 2022; Kummu et al., 2018) or the assumption that average building heights correlate with economic activity intensity (Taguchi et al., 2022).

While these studies estimated the total amount of economic losses without considering the difference between sectors, the sector-classified economic losses also need to be estimated because indirect economic losses, such as global supply chain impact caused by the stoppage of production activity (Willner et al., 2018), can vary significantly depending upon the sector directly affected by the flood (Sieg et al., 2019). However, spatial data of sectors by downscaling national-level data have been lacking. Consequently, in the context of global studies, the estimation of sector-specific losses was achieved by extrapolating the values of sectoral occupation fractions within urban area grids, as reported in the European Union, to other regions (Alfieri et al., 2016; Dottori et al., 2018). Alternatively, it is assumed that specific groups of sectors experience uniform damage ratios (Willner et al., 2018; Tanoue et al., 2020). These methods did not consider the different spatial accumulation between each sector and each region, which could lead to the misestimation of sector-classified losses (Jongman et al., 2012; Willner et al., 2018).

The dearth of global spatial data of the economic sector arises from the absence of worldwide maps with comprehensive land use categorizations (Wenz and Willner, 2022). While regional maps provide sectoral land use classifications, including commercial and industrial areas within urban regions (e.g., European Environmental Agency, 2017; Theobald, 2014; De Moel H et al., 2014; MLIT 2021), these classifications are conspicuously absent from global maps (e.g., Bontemps et al., 2011; Esch et al., 2017). Here we focused on the recent emergence of a global land use map featuring detailed urban area classifications (Pesaresi and Politis, 2022). This development is made possible by the application of machine learning techniques that extrapolate relationships between satellite observations and actual land uses, a methodology initially established by the data in the European Union and the United States (European Environmental Agency, 2017; Theobald, 2014) and subsequently extended to a global scale. Although this dataset facilitates a comprehensive consideration of

https://doi.org/10.5194/essd-2024-503
Preprint. Discussion started: 25 November 2024
© Author(s) 2024. CC BY 4.0 License.

detailed land-use patterns within urban areas worldwide, no study has yet integrated this dataset with socioeconomic data. Such integration holds the potential to pioneer a novel approach to estimating natural disaster damage accurately with sectoral classifications.

The objective of this study is to leverage a recently available global detailed land use map dataset to construct a spatially distributed sectoral GDP map. The accuracy of the distribution of economic sectors within this newly developed spatially distributed GDP map is evaluated using data from Thailand. Validation is achieved by scrutinizing the consistency of subnational statistics within Thailand. Furthermore, to discuss the applicability of the new GDP map for practical economic loss estimation, this study examines the estimation of business interruption losses incurred due to a flood event in Thailand and compares these estimations with reported values. The reason for choosing Thailand as a target of validation was that this country has both sectoral subnational GDP statistics and the reported values of sectoral economic losses caused by the historical event while most countries do not have nor publish those types of data.

2 Methods

2.1 Spatially distributed sectoral GDP map

The spatially distributed sectoral GDP map was created in two steps (Figure 1). First, we created a global sectoral land use fraction map at a spatial resolution of 30 arcsec, and combined satellite products to classify three sectors: the service, industry, and agricultural sectors. Then, country GDP data classified according to these sectors were distributed spatially on the corresponding sectoral area fractions in the global sectoral land use fraction map. The List of the datasets used in this method is shown in Table 1.

https://doi.org/10.5194/essd-2024-503
Preprint. Discussion started: 25 November 2024
© Author(s) 2024. CC BY 4.0 License.

Open Access Earth System Science Data Discussions

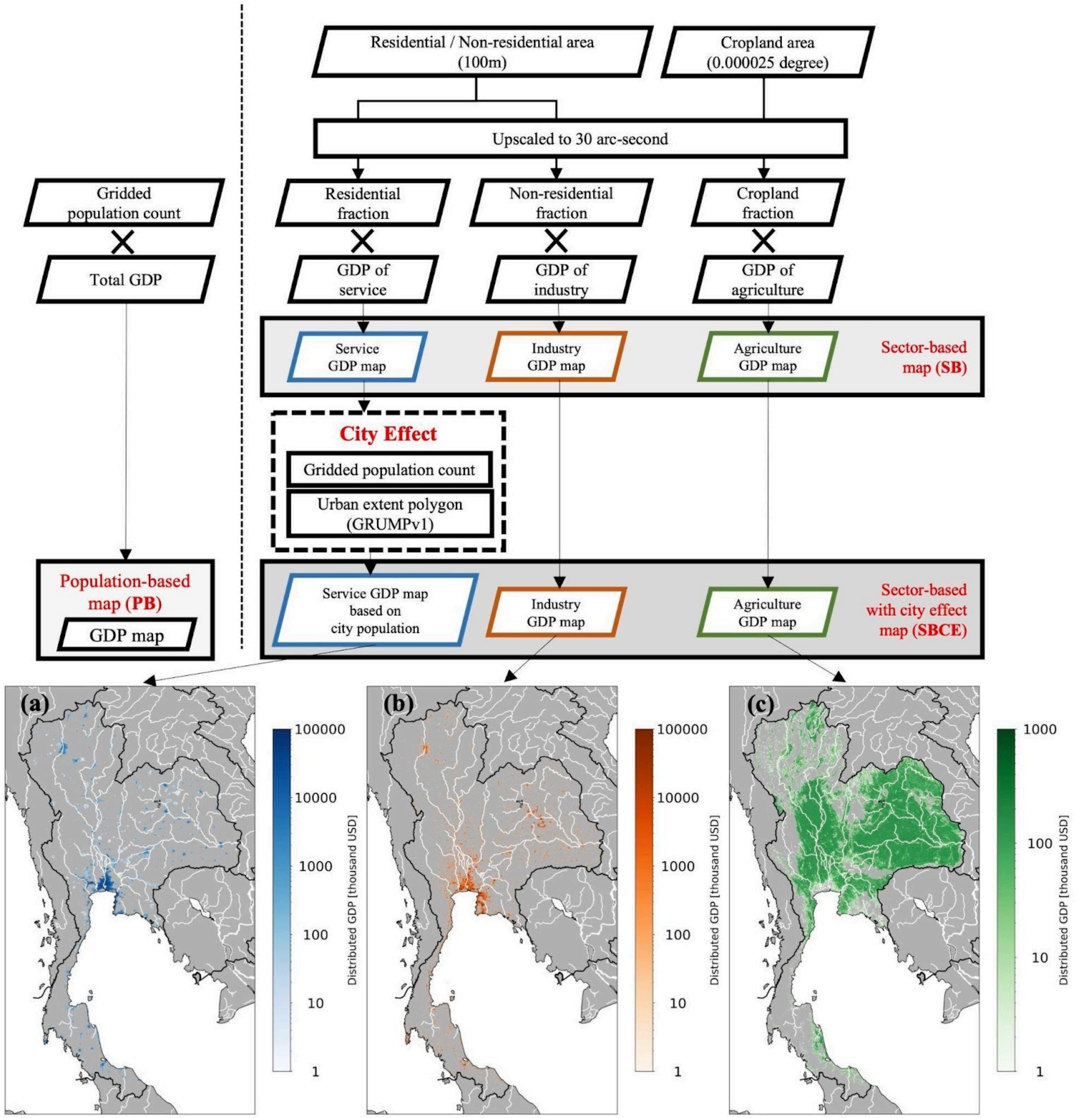

82

83 **Figure 1: Flowchart of (top) data processing and (bottom) creation of spatial distributed gross domestic product (GDP) maps of**
84 **Thailand for the (a) service, (b) industrial, and (c) agricultural sectors.**

85

https://doi.org/10.5194/essd-2024-503
Preprint. Discussion started: 25 November 2024
© Author(s) 2024. CC BY 4.0 License.
Open Access Earth System Science Data Discussions

Data	Format	Datatype	Values range	Spatial resolution	Temporal resolution	Data source, Reference
Built up surface area Non-residential surface area	Raster	UInt16	0-10000	100m	five years interval (1975-2020)	Global Human Settlement Layer (Pesaresi and Politis, 2022)
Crop land area	Raster	Boolean	0,1 (0 - no croplands, 1 - croplands)	0.9 arcsec	five years interval (2003-2019)	Potapov et al., 2022
Population count	Raster	Float64	0-Inf	30arcsec	five years interval (1975-2020)	Global Human Settlement Layer (Pesaresi and Politis, 2022)
City area polygons	Vector (Polygon)	-	-	-	-	Global Rural-Urban Mapping Project v1 (CIESIN, 2011)
Administrative units	Vector (Polygon)	-	-	-	-	GADM 4.1 (2023) Level 1 Layer

Table 1:List of the datasets used in this study.

In the first step, we used land use classification maps from satellite products to produce a global sectoral land use fraction map. We generated a sectoral land use fraction map classified into three sectors (service, industry, and agriculture) and three land use type maps with different spatial resolutions: residential (RES), non-residential (NRES), and cropland (CROP). To distinguish RES and NRES areas, we used Global Human Settlement Layer (GHSL) (Pesaresi and Politis, 2022) built-up surface (R2022) data. This layer has 100 × 100 m resolution; each pixel has a value of 0-10,000 m2 and residential or non-residential areas may be present within one pixel. For CROP area, we used the global map of cropland extent (Potapov et al., 2022), provided by Global Land Analysis & Discovery, which has a global spatial resolution of 0.9 arcsec. Maps with the three classes were resampled and combined into a single global sectoral land use (residential, non-residential, and cropland) fraction map at 30-arcsec resolution.

First, we upscaled the land use maps and simultaneously converted the value of each pixel in both maps into the sectoral fraction within one pixel. In each pixel, RES and NRES had values of 0–10000 m2 and CROP had a value of 0 or 1 (not cropland or cropland). We upscaled the land use maps to 30-arcsec resolution from RES and NRES at a resolution of 100 × 100 m and CROP at a resolution of 0.9 arcsec using the GDAL averaging method (GDAL/OGR contributors. 2024). Using the 30-arcsec maps, we calculated the area attributed to each land use type in one pixel with a size of 1 × 1 arcsec and obtained land use fractions for each pixel. Because RES/NRES and CROP had different data sources, the total of the three land use type fractions was greater than one in some pixels. Therefore, we assumed that the CROP fraction could fill only areas that were not designated as RES or NRES. Under this assumption, we modified the CROP fraction in each pixel as follows:

$$MCROP_i = min\left(CROP_i, \left(1 - RES_i - NRES_i\right)\right) \tag{1}$$

where $MCROP_i$ is the modified CROP fraction in pixel i, $CROP_i$ is the original CROP fraction, RES_i is the RES fraction, and $NRES_i$ is the NRES fraction.

https://doi.org/10.5194/essd-2024-503
Preprint. Discussion started: 25 November 2024
© Author(s) 2024. CC BY 4.0 License.

After this modification, RES, NRES, and MCROP were considered to represent the service, industrial, and agricultural land use sectors, respectively.

In the second step, we spatially distributed the country-level GDP onto the global sectoral land use fraction map generated in the first step. We used GDP data published by the World Bank (2023), which includes both yearly GDP values and their sectoral ratios for the service, industrial, and agricultural sectors. For industrial and agricultural GDP, we assumed that the sectoral GDP per area was the same in all the areas of that sector within each country; thus, the industrial and agricultural GDP were distributed only in proportion to the sectoral area fractions of each pixel, with a size of 30 × 30 arcsec.

To create a spatially distributed sectoral GDP map, we distributed the sectoral GDP into each sectoral land use area, in each country by multiplying the distributed sectoral GDP per pixel by the sectoral area fraction in each pixel. At this step, we assumed that the distributed sectoral GDP per pixel was the same only within the same country and the same sector. Thus, the distribution was performed for each country and each sector, as follows:

$$SGDP\ per\ pixel_{country,s} = \frac{TtlSGDP_{country,s}}{\sum_{i=1}^{n} SA\ fraction_{i,s}} \tag{2}$$

$$SGDP_{country,i,s} = SGDP\ per\ pixel_{country,s} \times SA\ fraction_{i,s} \tag{3}$$

where $SGDP\ per\ pixel_{country,s}$ is the sectoral GDP per pixel of sector s in the country, $TtlSGDP_{country,s}$ is the total sectoral GDP of sector s in the country, $SA\ fraction_{i,s}$ is the sectoral area fraction of sector s in pixel i, n is the total number of pixels in the country, and $SGDP_{country,i,s}$ is the distributed sectoral GDP of sector s in pixel i in the country.

For the service GDP distribution, the activity level in each service sector area depends strongly on the number of people living near that area and using services (Morikawa, 2011). Therefore, we considered the city effect only for the service sector. As an appropriate scale for counting the number of neighbors using the services of a specific area, the grid-scale population (e.g., 30-arcsec resolution, approximately 1 × 1 km per pixel) is too fine to describe a realistic number of users because many people often travel further than 1 km by car or public transportation. Country and district scales are too broad to reflect the intensity of demand of each area accurately (Ciccone and Hall, 1996). Additionally, population density corresponds more strongly to economic activity than to population counts (Ciccone and Hall, 1996; IMF, 2019). Therefore, we used city-scale population density information for the service sector GDP distribution (City Effect, Fig. 1).

The service GDP was distributed only in pixels within cities and the amount of distributed GDP was proportional to the population density of the city where the pixel is located. To detect pixels included in cities, we used the global city polygon dataset provided by Global Rural-Urban Mapping Project (GRUMP) v1 (CIESIN, 2011). To calculate the population density

https://doi.org/10.5194/essd-2024-503
Preprint. Discussion started: 25 November 2024
© Author(s) 2024. CC BY 4.0 License.

of each city, we used the global gridded population map provided by GHSL population grid (R2023; Pesaresi and Politis, 2022). For the distribution of service sector GDP, we first masked out the fractions of the service sector in pixels that did not belong to any city detected using the global city polygon dataset. We distributed GDP into only pixels that belonged to cities, and we assumed that the GDP per area was the same in one city and that the amount of gridded GDP was in proportion to the service sector fraction of each pixel. This calculation was performed as follows:

$$ServGDP\ per\ city_{country,city} = \frac{PD_{city}}{\sum PD_{city}} \times TtlServGDP_{country} \tag{4}$$

$$ServGDP\ per\ pixel_{country,city} = \frac{SectGDP\ per\ city_{country,city}}{\sum_{i=1}^{k} ServArea\ fraction_i} \tag{5}$$

$$ServGDP_{country,city,i} = ServGDP\ per\ pixel_{country,city} \times ServArea\ fraction_i \tag{6}$$

where $ServGDP$ is the service sector GDP, PD_{city} is the population density of the city, $TtlServGDP_{country}$ is the total amount of service sector GDP of the country, and $ServArea\ fraction_i$ is the fraction of service sector area in pixel i.

2.2 Comparison of GDP distribution methods

We created three types of spatial distributed GDP map: population-based (PB), sector-based (SB), and sector-based with City Effect (SBCE). The PB map was generated by downscaling the country GDP only in proportion to the gridded population count into a 30-arcsec map. The SB map was generated for each sectoral area and sectoral GDP per area, assuming that the sectoral GDP per area is the same within each country. The SBCE map was generated by considering the city-scale population density effect (City Effect) mentioned above, only for the service GDP distribution. The GDP of the industrial and agricultural sector in the SB map and the SBCE map were distributed using the same method.

3 Results

We developed three GDP maps for service, industry, and agriculture sectors in 2010, 2015, and 2020. We excluded other years because of the low coverage of national GDP statistics in the World Bank data. The developed sectoral GDP maps are shown in Fig. 2 (a), (b), and (c). Additionally, to clarify the difference of spatial distribution among sectors, we showed (d) the map of the largest GDP sector in each grid in the world and (e) around Thailand as an example. Although the GDP maps were produced with a spatial resolution of 30 arcsec, these maps in Fig. 2 show the aggregated maps into 0.5 degree. These GDP maps are those called SBCE in the Methods. Both maps of the service and industry sector showed the same shape of extents which have each sector GDP. Meanwhile, the GDP accumulation into the center of the economic activity was different between them. Looking at the east part of the United States, while industry GDP was scattered evenly in a wide

https://doi.org/10.5194/essd-2024-503
Preprint. Discussion started: 25 November 2024
© Author(s) 2024. CC BY 4.0 License.

area, service GDP accumulated intensely in some centers of cities and other areas have much smaller GDP in those places. This tendency was not the case with other countries. In countries such as India and Iran, the industry GDP was more concentrated in some specific areas than the service GDP. As for the agriculture GDP, compared to maps of those two sectors, the GDP was spread to a much wider area with less concentration in specific areas. Even with this different characteristic, the agriculture GDP was basically distributed aligning with the other two sectors' GDP. When we look at the map around Thailand (Fig. 2 (e)), we can see the different distribution between each sector. While the service GDP (blue) dominated in the Bangkok area, the industry GDP mainly dominated in the eastern area, next to the Bangkok area. The sectoral GDP map of this study showed such heterogeneity of each sector on a local scale within one country.

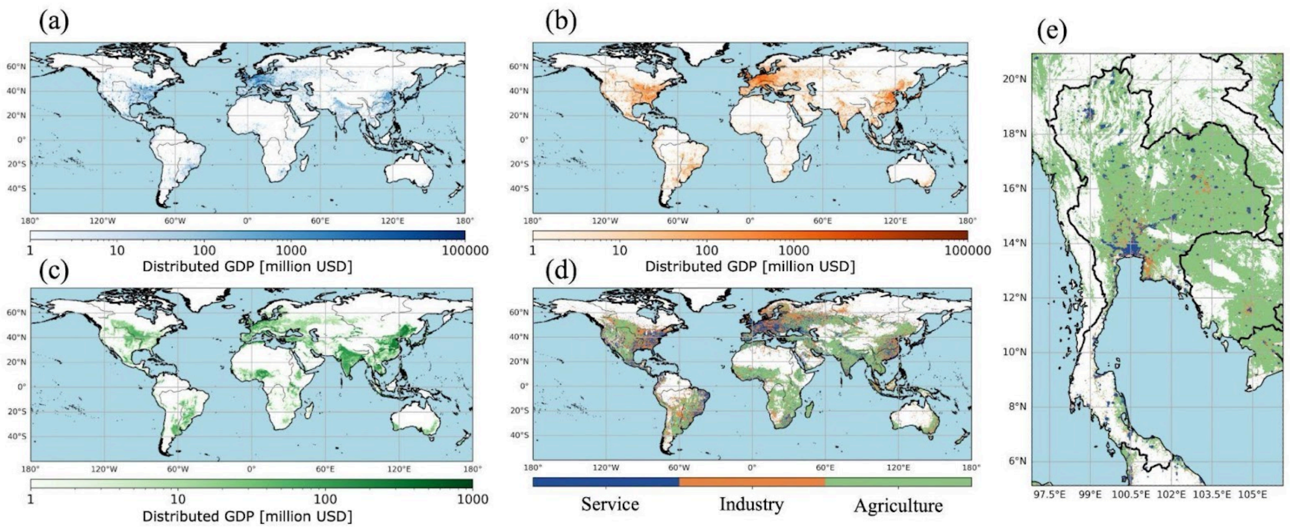

Figure 2: The sectoral GDP maps of (a) service sector, (b) industry sector, (c) agricultural sector, (d) the map of the largest GDP sector in each grid of 0.5 x 0.5 degree, and (e) the same map around Thailand.

We validated this different distribution of each sector's GDP using subnational sectoral GDP statistics of Thailand in 2009 provided by the Thailand government (NESDC, 2016) as reference data. We spatially aggregated the GDP map into seven districts corresponding to the statistics classification: Northeastern, Northern, Southern, Eastern, Western, Central, and Bangkok & Vicinity (Fig. 3). This aggregation was performed using the administrative area polygon dataset obtained by GADM 4.1 (2023) and its correspondence with the district definition in the statistics. The spatially aggregated GDP of each sector in each district of the three maps (PB, SB, SBCE) and the Thailand government statistical values (Reference) are shown in Fig. 3. The population-based map had no information on sectoral differences among districts; therefore, the sectoral ratio of the gridded GDP value was assumed to match that of the entire country in all pixels and districts, following the practice of previous studies (Willner et al., 2018; Tanoue et al., 2020). As an index of consistency of the three maps with

https://doi.org/10.5194/essd-2024-503
Preprint. Discussion started: 25 November 2024
© Author(s) 2024. CC BY 4.0 License.

Reference, we calculated average relative errors (ARE) of the aggregated district GDP in each map to Reference, on an average of all seven districts, as follows:

$$ARE[\%] = \frac{1}{7}\sum_{k=1}^{7}\left|\frac{Regional\ GDP_k - Ref_k}{Ref_k}\right| \times 100 \qquad (7)$$

where k is the number of each district shown in Fig. 3.

The AREs for the total GDP values of the PB, SB, and SBCE maps were 63.0%, 50.0%, and 26.2%, respectively. These AREs consisted of errors of each sector in each district. For the service sector, the AREs were 50.3%, 69.2%, and 38.6%, respectively, in the PB, SB, and SBCE map. The largest service GDP was seen in Bangkok & Vicinity in Reference. While it was seen in the same district in the SBCE map, the different district (Southeastern) had the largest in the other two maps (PB and SB). This result meant the SBCE showed better consistency with Reference than PB and even SB. This indicated that solely using the residential fraction map was not enough to express the spatial distribution of service GDP and the city-scale population density could help to reproduce the actual GDP distribution.

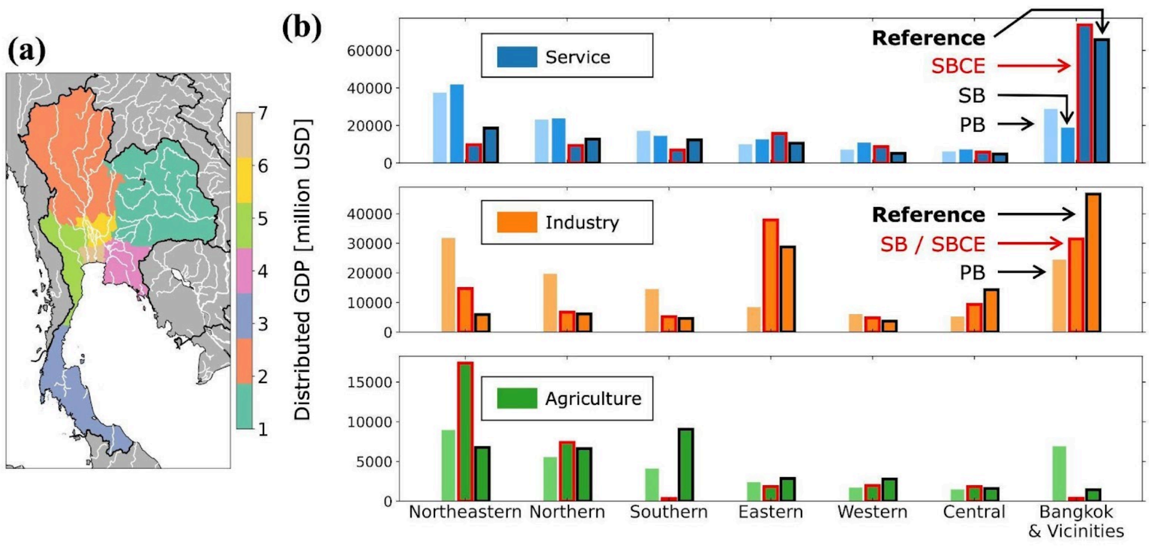

Figure 3: (a) The seven districts of Thailand (1, Northeastern; 2, Northern; 3, Southern; 4, Eastern; 5, Western; 6, Central; 7, Bangkok and Vicinities). (b) Distributed sectoral GDP of subnational even districts in Thailand in 2009, obtained from the population-based (PB), sectoral-based with city effect (SBCE) maps and statistical values from the government of Thailand (Reference).

For the industrial sector, the AREs were 159% and 42.7% in the PB and SB/SBCE map, showing the PB map had a marked inconsistency to Reference. On the other hand, SB/SBCE maps could express the large industry GDP in districts such as

https://doi.org/10.5194/essd-2024-503
Preprint. Discussion started: 25 November 2024
© Author(s) 2024. CC BY 4.0 License.

Eastern and Central. This indicated that the accumulation of non-residential fraction, which was hypothetically assumed to correspond to industry GDP in this study, corresponded well with the distribution of industry sector activities.

Conversely, for the agriculture sector, which was spatially distributed using the same method as for the industrial sector, none of the three maps could show the largest agriculture GDP in the Southern district. The SB/SBCE map showed an overestimation in Northeastern and underestimation in Southern and Bangkok & Vicinity. This indicated that the cropland fraction map used in the Method could not express the intense accumulation of agriculture GDP. The cropland map used in this study has no information on crop types; thus, the productivity of individual crop types was ignored for each district in Thailand. For example, the Northeastern district produces mainly rice with low land productivity, whereas the Southern district produces natural rubber and palm oil (Inoue, 2010). This heterogeneity of "production in monetary unit per area" was not considered in this study, which probably led to the low improvement of GDP distribution accuracy in the SB/SBCE map.

4 Discussion

4.1 Business interruption loss estimation for the 2011 Thailand flood

To assess how the improvement of the GDP map affects the result of flood loss estimation, an additional analysis of estimating business interruption losses resulting from the actual flood event in Thailand in 2011 by the new sectoral GDP map was conducted to assess how the improvement of the GDP map affects the result of flood loss estimation. Following established definitions of economic losses from prior studies (Tanoue et al., 2020; Rose, 2004), economic impacts can be categorized into three main types: damage, direct economic loss, and indirect economic loss. This additional analysis focused exclusively on estimating BI loss among these three economic impacts due to the lack of information necessary for the estimation of the other components.

To calculate BI loss, we prepared hazard, exposure, and vulnerability data. As the hazard, we used two inundation period maps of the target event in Thailand, based on simulation and satellite observations. The simulation-based inundation period map was generated using the Catchment-based Macro-scale Floodplain (CaMa-Flood) global riverine inundation model (Yamazaki et al., 2011). To obtain an inundation map based on the simulation by CaMa-Flood, CaMa-Flood used daily runoff data generated by a reduced-bias meteorological forcing dataset at 15-arcmin resolution, and S14FD-Reanalysis data (Iizumi et al., 2017) to simulate the daily inundation depth at 15-min resolution. Because S14FD is a bias-corrected dataset, we used daily inundation depth values without bias correction, such that the inundation period may be calculated directly from the daily inundation depth (Taguchi et al., 2022). Then, we downscaled the 15-arcmin daily inundation depth to 30-arcsec resolution and calculated the inundation period as the number of days in which the inundation depth exceeded 0.5 m in each pixel. We also used an inundation period map based on Terra/Moderate Resolution Imaging Spectroradiometer

https://doi.org/10.5194/essd-2024-503
Preprint. Discussion started: 25 November 2024
© Author(s) 2024. CC BY 4.0 License.

(MODIS) images, which is publicly available on the Global Flood Database (Tellman et al., 2021). We referred to the former hazard map as “CaMa-Flood” and the latter map as “MODIS” in this study. The days between August and December in 2011 were only counted as inundation days for matching the inundation period by CaMa-Flood simulation and that by MODIS observation, which started from August and ended around the end of December. The inundation period maps of CaMa-Flood and MODIS are shown in Fig. 4.

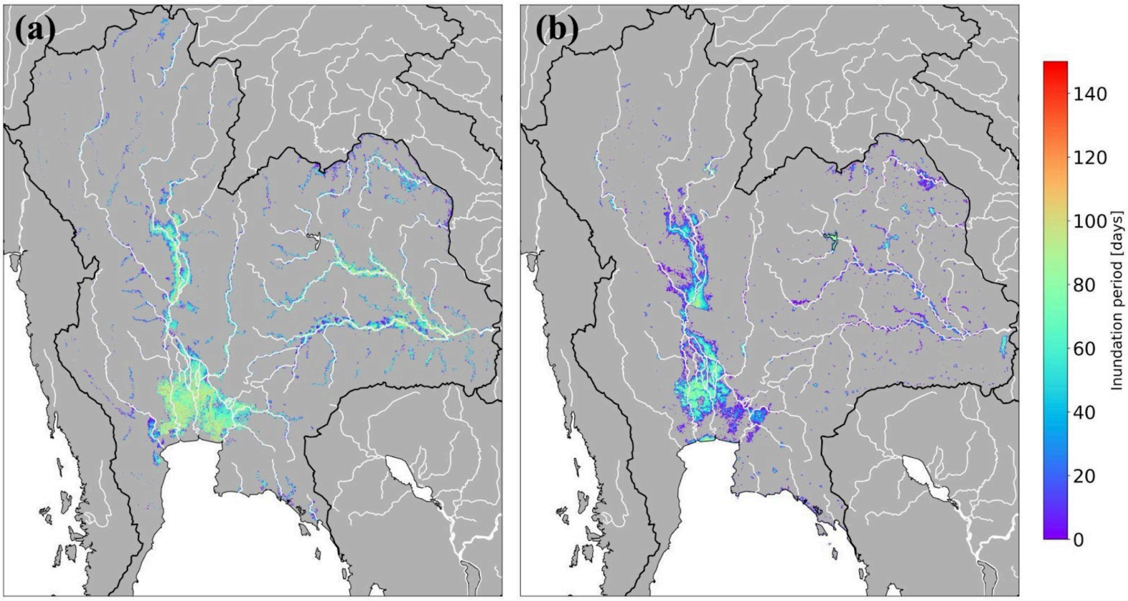

Figure 4: Spatial distribution of the inundation period of the 2011 Thailand flood, obtained from (a) Catchment-based Macro-scale Floodplain (CaMa-Flood) simulation and (b) Moderate Resolution Imaging Spectroradiometer (MODIS) observation data.

As exposure, we used two spatial distributed GDP maps at 30-arcsec resolution for comparison, the population-based map (PB) and the sector-based map with CE (SBCE). As a vulnerability, we considered a recovery coefficient, which decided the ratio of the length of recovery period which is required until business restart to the inundation period. This value reflects the system vulnerability of the city. We used 2 as a recovery coefficient, which was used in previous study on a global scale (Taguchi et al., 2022). As for the recovery period as vulnerability, we used the method of Tanoue et al. (2020). The recovery period RP_i, when the production in a pixel is assumed to have recovered linearly from zero at the end of the flood period to the same level of production before the flood, was obtained by multiplying the inundation period by a coefficient (= 2 in this study). Thus, the recovery period was assumed to take twice as long as the inundation period. Finally, BI loss was estimated by the method described by Tanoue et al. (2020), as follows:

$$BI\ loss = \sum_{i=1}^{N} \sum_{s}^{3} \left\{ (IP_i + \frac{RP_i}{2}) \times \frac{AGDP_{i,s}}{Nd} \right\} \quad (8)$$

https://doi.org/10.5194/essd-2024-503
Preprint. Discussion started: 25 November 2024
© Author(s) 2024. CC BY 4.0 License.

where i, N, and s are the pixel number, total number of pixels in the inundated area, and sector number (1 = service, 2 = industry, and 3 = agriculture), respectively; IP_i, RP_i, $AGDP_{i,\,s}$, and Nd are the inundation period, recovery period at pixel i, annual GDP of pixel i and sector s, and the number of days in a year.
And we obtained the total BI losses by summing BI losses of all the grids in the target area.

The results of the BI loss estimation were shown in Fig. 5. We compared the calculated BI losses with the actual economic loss reported in the PDNA (The World Bank, 2011). In this report, both damage and loss were estimated. Damage is due to the destruction of physical assets and loss is caused by foregone production and income and higher expenditures in the definition in the report. This means that the loss in the report included both business interruption loss and other additional expenditures and costs. Because there was not any other reported loss which only focused on BI loss, we compared with the loss, including other components, in this report.

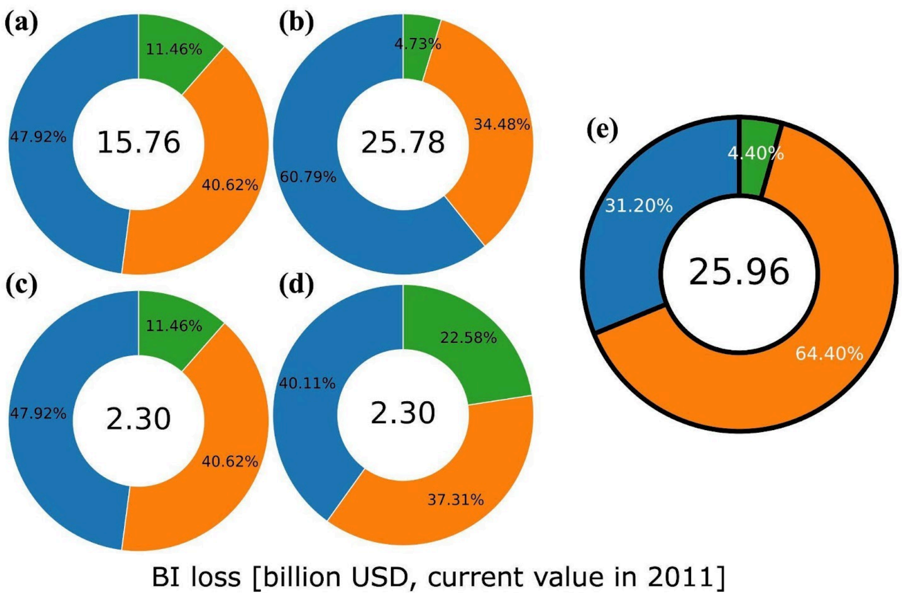

Figure 5: Business interruption losses (USD billion, current value in 2011) due to the 2011 Thailand flood, estimated by combining hazards and exposures; the total loss is written in the center of each circle. (a) CaMa-Flood and population-based map (PB), (b) CaMa-Flood and sectoral-based map with city effect (SBCE), (c) MODIS and population-based map (PB), (d) MODIS and sector-based map with city effect (SBCE), and (e) the World Bank report (2011).

Firstly, comparing the losses by the different hazard data with the same exposure, the SBCE map, the service sector loss according to CaMa-Flood (USD 15.67 billion) was over 15-fold larger than that according to MODIS (USD 0.92 billion). This large difference was caused by the shorter average inundation period and smaller flood area in MODIS than in CaMa-Flood. MODIS is known to tend to fail to capture the flood extent in urban areas with high densities of tall buildings

https://doi.org/10.5194/essd-2024-503
Preprint. Discussion started: 25 November 2024
© Author(s) 2024. CC BY 4.0 License.

Open Access Earth System Science Data Discussions

and that leads to the underestimation in inundation. In addition to different total losses, ratios of service sector loss to the total loss differed between two results : 60.79% according to CaMa-Flood and 40.11% according to MODIS. This result showed the sectoral ratio of the loss can be changed depending on spatially different hazards. This sectoral difference was newly found by this study since the traditional population-based GDP map could not show this difference.

The result by the set of hazard of CaMa-Flood and exposure of the SBCE map (b in Fig. 5) was consistent with the reported total loss, although the sectoral losses differed from the report. The total loss differed from the report by only –0.72% (USD 25.78 billion estimated loss vs. USD 25.96 billion reported loss), the service sector loss was overestimated (USD +7.57 billion loss, +29.59 point sectoral loss ratio), and the industrial sector loss was underestimated (USD –7.83 billion loss, –29.92 point sectoral loss ratio). In the service sector, the results were overestimated for the larger inundation extent and longer inundation period due to the lack of flood protective effect data in urban areas, where many services are located. In the industrial sector, although the hazard in the numerical simulation captured the flood extent over the industrial sector area and the long-lasting inundation period, the loss was underestimated. The reported value excludes assets damage but includes economic losses other than production reduction by direct contact with the flood, such as production stoppage due to shortages of raw materials induced by blocked roads. Therefore, if we assume that the new sectoral GDP map captured the industrial locations and they were successfully considered to be flooded, this underestimation is presumed to be caused by a lack of data reflecting the indirect production stoppage.

In addition to the notable omissions of urban flood protection and indirect production stoppage from the analysis, addressing the inherent uncertainty associated with the recovery coefficient is of utmost importance. This coefficient plays a pivotal role in calculating the recovery period following an inundation event and consequently has a substantial impact on the estimation of business interruption losses, as demonstrated in the equation. However, determining the most appropriate coefficient proves to be a formidable challenge, given its variability across different locations and sectors, a fact substantiated by both Taguchi et al. (2022) and Kimura et al. (2007). Presently, attempting to ascertain the ideal coefficient for each sector is difficult due to the absence of comprehensive observed data. It is crucial that future research investigates this matter.

4.2 Limitation

Firstly, there are uncertainties in the assumption of distributing sectoral GDP in proportion to the fraction of each land use. In the Methods, we decided to consider the other components affecting the spatial accumulation such as population density only in service GDP and assumed GDP per area is uniform in industry and agriculture. However, GDP per area could be different depending on areas. For agriculture, it was indicated that GDP per area depends on the type of crops in the Result. Also, for industry, produce per area was reported as different depending on sub sectors among industry. For example, in Japan, production per area of the chemical products sector is almost five times larger than that of transport equipment (METI, 2007). These indications are difficult to utilize for the method of generating the global map because the data related to spatial distribution of crop type and subsectors are not available, which is the different case from the service GDP map using globally available population map. In this study, we indicated the importance of considering other components affecting GDP per area by showing the improvement of service GDP map by City Effect and the low accuracy of agriculture GDP map. Therefore, we expected further research on finding relationships between sectoral GDP per area and indices which could be obtained by public and globally available data such as those provided by satellite observation or public statistics.

This study was limited in that the validation and comparison of the GDP map was performed only for Thailand and for the map in 2010. The study methodology should be validated for other countries prior to global applications. However, this is the first study to quantify the differences between traditionally used GDP maps and actual economic activity, and to evaluate how such GDP maps may be improved using satellite products, for countries with large differences in sectoral GDP among subnational districts, such as Thailand. In this point, this study could contribute to the improvement of global natural hazard risk assessment, as the methodology and dataset used in this study can be easily applied to global. For that this study investigated only the map in 2010, although we did not carry out the analysis on the temporal change of sectoral GDP map, the data of land use map and national sectoral GDP we used in this study are available in other multiple years. Thus, the method in this study is applicable also to the analysis on different time series and we expected further analysis on it in the future.

5 Data availability

The global sectoral GDP maps are publicly available via Zenodo at https://doi.org/10.5281/zenodo.13991673 (Shoji et al., 2024). The maps on Zenodo correspond to the SBCE maps in this paper and are stored as geotiff files. In total, there are nine maps in the dataset, for each sector (service, industry, and agriculture) and year (2010, 2015, and 2020).

6 Summary

In this study, we generated a spatially distributed sectoral GDP map by leveraging a recently available global detailed land use dataset; the map showed better consistency with subnational GDP statistics than the traditional GDP map did, relying only on the gridded population map. We found that the land use classification of residential and non-residential areas could be used to spatially distinguish the service and industrial sector areas. The accumulation of non-residential areas worked well as a proxy of industrial sector production intensity. Conversely, that of residential areas was insufficient to express the high accumulation of economic activity by the service sector in large cities. To overcome this problem, we considered the city-scale effect of the intensity of service sector production. This city-scale effect expressed a realistic economic activity

https://doi.org/10.5194/essd-2024-503
Preprint. Discussion started: 25 November 2024
© Author(s) 2024. CC BY 4.0 License.

accumulation in the service GDP distribution and is a globally available satellite product. For the agricultural sector, we determined that it is necessary to incorporate crop type information.

The flood BI loss estimation using the sector-based GDP map confirmed that the new sectoral GDP map was able to express sectoral differences in the estimated BI loss, depending on the different spatial distributions of hazard. The underestimation of the industrial sector loss was probably resulting from a lack of data reflecting the effect of transportation network disruption. To consider the loss due to such transportation disruption and estimate more realistic economic losses, it is necessary to include information on both the road network and transportation of goods for the industrial sector by combining road network data and transportation statistics between each area within each country.

This new sectoral GDP map in global can serve as a foundation for estimating economic losses classified by sector while meticulously accounting globally for the intricacies of land use patterns. This enables precise calculations of sector-specific losses by various natural hazards on a global scale.

Competing interests

The contact author has declared that none of the authors has any competing interests.

Acknowledgement

This work was supported by Japan Science and Technology Agency (JST) [Moonshot R&D; JPMJMS2281] and Ministry of the Environment of Japan / Environmental Restoration and Conservation Agency [Development Fund; JPMEERF23S21130].

References

Alfieri L, Bisselink B, Dottori F, Naumann G, De Roo A, Salamon P, Wyser K, Feyen L.: Global projections of river flood risk in a warmer world. Earth's Future 5: 171-182, 2017.

Bontemps S, Herold M, Kooistra L, Van Groenestijn A, Hartley A, Arino O, Moreau I, Defourny P.: Revisiting land cover observations to address the needs of the climate modelling community. Earth System Science/Response to Global Change: Climate Change, Preprint Report, 2011.

https://doi.org/10.5194/essd-2024-503
Preprint. Discussion started: 25 November 2024
© Author(s) 2024. CC BY 4.0 License.

Ciccone A, Hall RE.: Productivity and the density of economic activity. The American Economic Review 86: 54–70. http://www.jstor.org/stable/2118255, 1996.

CIESIN (Center for International Earth Science Information Network).: Global Rural-Urban Mapping Project, Version 1 (GRUMPv1): Urban Extent Polygons, v1.02, 2011.

De Moel H, Van Vliet M, Aerts JCJH.: Evaluating the effect of flood damage-reducing measures: a case study of the unembanked area of Rotterdam, the Netherlands. Regional Environmental Change 14: 895–908, 2014.

Dottori F, Szewczyk W, Ciscar J, Zhao F, Alfieri L, Hirabayashi Y, Bianchi A, Mongelli I, Frieler K, Betts RA, Feyen L.: Increased human and economic losses from river flooding with anthropogenic warming. Nature Climate Change 8: 781-786, 2018.

Duan Y, Xiong J, Cheng W, Li Y, Wang N, Shen G, Yang J.: Increasing Global Flood Risk in 2005–2020 from a Multi-Scale Perspective. Remote Sensing 14: 5551, 2022.

Esch T, Heldens W, Hirner A, Keil M, Marconcini M, Roth A, Zeidler J, Dech S, Strano E.: Breaking new ground in mapping human settlements from space – The Global Urban Footprint. ISPRS Journal of Photogrammetry and Remote Sensing 134: 30-42, 2017.

GADM 4.1. https://gadm.org/.

GDAL/OGR contributors.: GDAL/OGR Geospatial Data Abstraction software Library. Open Source Geospatial Foundation. https://gdal.org, 2024.

Hirabayashi Y, Mahendran R, Koirala S, Konoshima L, Yamazaki D, Watanabe S, Kim H, Kanae S.: Global flood risk under climate change. Nature climate change 3: 816-821, 2013.

Huizinga J, De Moel H, Szewczyk W.: Global flood depth-damage functions: methodology and the database with guidelines. European Commission, Joint Research Centre, 2016.

Iizumi T, Takikawa H, Hirabayashi Y, Hanasaki N, Nishimori M.:Contributions of different bias-correction methods and reference meteorological forcing data sets to uncertainty in projected temperature and precipitation extremes. Journal of Geophysical Research-Atmospheres, 2017.

IMF.: How Should We Measure City Size Theory and Evidence Within and Across Rich and Poor Countries. IMF: Washington, DC, USA. https://www.imf.org/en/Publications/WP/Issues/2019/09/20/How-Should-We-Measure-City-Size-Theory-and-Evidence-Within-and-Across-Rich-and-Poor-Countries-48671, 2019.

Inoue S.: Agriculture and its Policy in Thailand. MAFF (Ministry of Agriculture, Forestry and Fisheries). https://www.maff.go.jp/primaff/koho/seminar/2010/attach/pdf/101026_01.pdf. (In Japanese), 2010.

IPCC.: Managing the Risks of Extreme Events and Disasters to Advance Climate Change Adaptation. A Special Report of Working Groups I and II of the Intergovernmental Panel on Climate Change: 582 pp, 2012.

https://doi.org/10.5194/essd-2024-503
Preprint. Discussion started: 25 November 2024
© Author(s) 2024. CC BY 4.0 License.

Jongman B, Kreibich H, Apel H, Barredo JI, Bates PD, Feyen L, Gericke A, Neal J, Aerts JCJH, Ward PJ.: Natural Hazards and Earth System Sciences 12: 3733-3752, 2012.

Jovel RJ, Mudahar M.: Damage, loss, and needs assessment guidance notes: Volume 3. Estimation of post-disaster needs for recovery and reconstruction. Washington, DC, Report. http://hdl.handle.net/10986/19046, 2010.

Kimura S, Ishikawa Y, Katada T, Asano K, Sato H.: The structural analysis of economic damage of offices by flood disasters in urban areas. Japanese Journal of JSCE 63: 88-100 (in Japanese), 2007.

Koks EE, Bočkarjova M, De Moel H, Aerts JCJH.: Integrated Direct and Indirect Flood Risk Modeling: Development and Sensitivity Analysis: Integrated Direct and Indirect Flood Risk Modeling. Risk Analysis 35: 882-900, 2015.

Kummu M, Maija T, Guillaume JHA.: Gridded global datasets for gross domestic product and human development index over 1990–2015. Scientific Data 5: 180004, 2018.

Ministry of Economy, Trade, and Industry.: A survey on industry statistics. https://www.meti.go.jp/statistics/tyo/kougyo/result-2/h10/kakuho/youti/youti1.html, 2007.

Ministry of Land, Infrastructure, Transport and Tourism.: Mesh Data of Subdivided Land Use in Urban Area. https://nlftp.mlit.go.jp/ksj/gml/datalist/KsjTmplt-L03-b-u.html, 2021.

Morikawa M. Economies of density and productivity in service industries: An analysis of personal service industries based on establishment-level data. Review of Economics and Statistics 93: 179–192, 2011.

NESDC (Office of the National Economic and Social Development Council, Thailand).: Gross Provincial Product 1995–2009 (16 sectors). https://www.nesdc.go.th/main.php?filename=gross_regional, 2016.

Pesaresi M, Politis P.: GHS-BUILT-S R2022A: GHS built-up surface grid, derived from Sentinel2 composite and Landsat, multitemporal (1975–2030). European Commission, Joint Research Centre (JRC), 2022.

Potapov P, Svetlana T, Matthew CH, Alexandra T, Viviana Z, Ahmad K, Xiao-Peng S, Amy P, Quan S, Jocelyn C.: Global maps of cropland extent and change show accelerated cropland expansion in the twenty-first century. Nature Food 3: 19–28, 2022.

Rose A.: Economic Principles, Issues, and Research Priorities in Hazard Loss Estimation. Modeling Spatial and Economic Impacts of Disasters, Springer Berlin Heidelberg, Berlin, Heidelberg; 13-36, 2004.

Shoji T, Yamazaki D, Kita Y, Megumi W.: Global Sectoral GDP map at 30" resolution (SectGDP30) v1.0, https://doi.org/10.5281/zenodo.13991673, 2024.

Sieg T, Thomas S, Kristin V, Reinhard M, Bruno M, Heidi K.: Integrated assessment of short-term direct and indirect economic flood impacts including uncertainty quantification. PLOS ONE 14: e0212932, 2019.

Taguchi R, Tanoue M, Yamazaki D, Hirabayashi Y.: Global-scale assessment of economic losses caused by flood-related business interruption. Water 14: 967, 2022.

Tanoue M, Hirabayashi Y, Ikeuchi H.: Global-scale river flood vulnerability in the last 50 years. Scientific Reports 6: 36021, 2016.

https://doi.org/10.5194/essd-2024-503
Preprint. Discussion started: 25 November 2024
© Author(s) 2024. CC BY 4.0 License.

Tanoue M, Taguchi R, Nakata S, Watanabe S, Fujimori S, Hirabayashi Y.: Estimation of direct and indirect economic losses caused by a flood with long-lasting inundation: Application to the 2011 Thailand flood. Water Resources Research 56, 2020.

Tanoue M, Taguchi R, Alifu H, Hirabayashi Y.: Residual flood damage under intensive adaptation. Nature Climate Change 11: 823-826, 2021.

Tellman B, Sullivan JA, Kuhn C, Kettner AJ, Doyle CS, Brakenridge GR, Erickson TA, Slayback DA.: Satellite imaging reveals increased proportion of population exposed to floods. Nature 596: 80–86, 2021.

The European Environmental Agency.: CORINE Land Cover. https://land.copernicus.eu/en/products/corine-land-cover?tab=main, 2017.

Theobald DM.: Development and Applications of a Comprehensive Land Use Classification and Map for the US. PLoS ONE 9: e94628, 2014.

Wenz L, Carr RD, Kögel N, Kotz M, Kalkuhl M.: DOSE – Global data set of reported sub-national economic output. Sci Data 10: 425, 2023.

Wenz L, Willner SN.: 18. Climate impacts and global supply chains: An overview. Handbook on Trade Policy and Climate Change, 290, 2022.

Willner SN, Otto C, Levermann A.: Global economic response to river floods. Nature Climate Change 8: 594–98, 2018.

The World Bank.: 2011 Thailand Floods: Rapid Assessment for Resilient Recovery and Reconstruction Planning. https://recovery.preventionweb.net/publication/2011-thailand-floods-rapid-assessment-resilient-recovery-and-reconstruction-planning, 2011.

The World Bank.: World Development Indicators. https://databank.worldbank.org/source/world-development-indicators, 2023.

Yamazaki, D, Kanae S, Kim H, Oki T.: A physically-based description of floodplain inundation dynamics in a global river routing model: FLOODPLAIN INUNDATION DYNAMICS. Water Resources Research 47: w04501, 2011.